Effects of abnormal paddy feeding states on the contact mechanical properties of rubber rollers in rice hullers

Min Cheng[1*], Shihao Zhou[2], Yong Pan[3], Haocong Meng[1], Xingchuang Wang[1], Xianzhou Cao[1]

(1. *School of Mechanical and Electrical Engineering, Henan University of Technology, Zhengzhou 450001, China*;
2. *Chery Commercial Vehicle (Anhui) Co., LTD. Henan branch, Kaifeng 475008, Henan, China*;
3. *School of Intelligent Engineering, Henan Mechanical and Electrical Vocational College, Zhengzhou, 451191, China*)

Abstract: Aiming at the problem of uneven wear of rubber rollers in rice hullers, this work systematically revealed the influence mechanism of abnormal paddy flow states on the contact mechanical properties of rubber rollers based on a nonlinear finite element model of the interaction between paddy grains and rubber rollers. The results show that the wear risk of rubber rollers is minimized when the paddy orientation angle ranges from 0° to 15°. At 30°, the contact pressure reaches 12.63 MPa with a sharp increase. At 45°, shear-dominated loading results in a peak von Mises stress of 2.70 MPa, with unsatisfactory rubber roller wear and hulling rate. Paddy orientation angles from 60° to 90° lead to slight rubber roller wear. With a sparse paddy distribution, 3 paddy grains induce shear fatigue in the middle of the rubber roller, whereas 5 grains result in a contact pressure of 7.09 MPa, which can cause local rubber layer detachment. Although 6 paddy grains exhibit the lowest wear risk among sparse distribution conditions, their dynamic stability is poor. Conversely, a dense distribution of 12 paddy grains results in a contact pressure of 6.92 MPa with a time difference of 0.2 ms, featuring a more uniform stress distribution and superior dynamic synchrony. Paddy stacking causes high contact pressure and von Mises stress (up to 13.85 MPa and 5.44 MPa respectively), which is the primary cause of crack initiation and local spalling on rubber rollers. The mechanical performance of stacked paddy flow is far inferior to that of sparsely and densely distributed paddy flows, which will inevitably cause uneven wear of the rubber rollers. This study provides theoretical support for reducing uneven wear of rubber rollers and improving paddy processing efficiency.

Keywords: rubber roll huller, uneven wear, abnormal paddy flow, nonlinear finite element, contact pressure, von Mises stress

DOI: 10.25165/j.ijabe.20261901.10272

1 Introduction

As the core working component of a huller, the normal operation and stable wear of the rubber roller are crucial for achieving the hulling process effect and improving processing efficiency[1,2]. Currently, the cleaning process can enhance the purity of the paddy material flow, while the impurity removal process can further eliminate substandard particles and foreign objects[3-5]. Meanwhile, the application of a vibrating feeding system helps realize the continuous and uniform supply of paddy[6]. In practical paddy husking production, the variability of raw materials and operational conditions often leads to uneven grain distribution states such as sparse, stacked, or inclined distributions. This results in uneven stress distribution on the rubber rolls and accelerates

localized wear, ultimately compromising process efficiency and equipment performance. Therefore, revealing the intrinsic relationship among paddy flow, stress distribution, and wear progression is pivotal to accurately predicting and mitigating uneven wear of rubber rolls.

Currently, the interaction between the distribution state of rolled paddy and the surface of the rolls is not sufficiently studied, but some scholars have carried out exploratory research around the relevant influencing factors in the paddy processing process. Chen et al.[7] and Firouzi et al.[8] investigated the effects of feeding angle and paddy moisture content on the hulling performance, respectively. They found that with the increase in feeding angle, the hulling rate showed a linear downward trend; and as the paddy moisture content increased, the hulling rate also decreased. Chen et al.[9] further investigated the effect of the inclined angle of the long flow plate on paddy flow, and found that the uniformity of paddy inclination decreases with the increase of the flow plate angle. To analyze the mechanism of preferred orientation of paddy flow, Fei et al.[10] studied the preferred orientation behavior of paddy grains using the Discrete Element Method (DEM). The results showed that under the action of velocity fluctuations, paddy grains tend to arrange horizontally to achieve the most stable state. On the other hand, regarding the effect of paddy variety on hulling rate, Shitanda et al.[1] found that its effect on the shelling rate is weak. As for the factors affecting the wear of rubber rollers, Prabhakaran et al.[11] clearly stated that the wear of rubber rollers is determined by the pressure of rubber rollers, feed rate, and line speed difference. Wang et al.[12] further quantified the impact of the rotational speeds

of the fast and slow rubber rollers and their linear speed difference on dehulling efficiency through simulation. To address the real-time monitoring and compensation of rubber roller wear, Wu et al.[13] developed a three-dimensional online detection algorithm based on point cloud data, providing a new technical means for the intelligent management of roller health status. In terms of rubber roller material selection, Adisa et al.[14,15] explored the effectiveness of industrial rubber and Teflon as rubber roller materials for hulling operations and showed that industrial rubber can be used as a rubber roller material as an alternative to PTFE. In addition, rubber rollers with different degrees of softness and hardness have a greater impact on hulling performance, soft rubber rollers are prone to rolling loss due to the sharp corners of paddy, while harder rubber rollers have a higher hulling rate at lower positive pressures but cause an increase in paddy crushing rate[7,16,17]. In terms of rubber roller gap control, Alwan et al.[18] showed that when the rubber roller gap is reduced, the hulling rate, crushing rate, and cracking rate show an increasing trend. However, under specific conditions, such as choosing a reasonable rubber roller gap of 0.8 mm and keeping the moisture content of paddy in a suitable range of 10%-12%, it can ensure that the paddy achieves the best hulling effect and effectively controls the crushing rate[19,20].

Existing research methodologies exhibit inherent limitations: Hertz Contact Theory struggles to model dynamic multi-particle coupling[21]; the Discrete Element Method (DEM) lacks sufficient accuracy in simulating continuous rubber roll deformation and stress fields[22]; whereas single-shelling tests can directly reflect the impact of process parameters on shelling performance, their results are constrained by specific test environments and equipment. These limitations have hindered the establishment of a cross-scale coupling model capable of integrating "paddy distribution-rubber roll deformation-contact stress", thereby preventing a systematic explanation of the mechanical essence underlying how uneven flow induces uneven rubber roll wear. To address this, this work proposes an analytical framework based on the nonlinear finite element method. Its innovation lies in directly modeling uneven feeding states, overcoming previous simplifying assumptions. By introducing a multi-indicator evaluation system comprising maximum contact pressure, maximum von Mises stress, and the time difference between their peak occurrences, this study, for the first time, reveals the quantitative relationship between uneven flow and the non-uniform stress and wear evolution of rubber rolls. Consequently, it provides a theoretical basis for predicting and mitigating uneven rubber roll wear from a fundamental mechanical perspective.

2 Establishment of a nonlinear contact model between paddy grains and rubber rollers

2.1 Theoretical assumptions

To investigate the contact mechanical characteristics between the uneven paddy grain flow and the rubber rollers, the following assumptions need to be made during the simulation process:

1) Assuming paddy grains form a monolayer on the rubber roll surface, with stacked grains simplified as "particle clusters", this assumption may weaken the representation of complex force transmission between stacked grains and could underestimate locally extreme pressure. However, it retains clear mechanistic value for revealing the wear formation mechanism driven by the core factor of "uneven distribution".

2) It is assumed that all paddy grains are rigid bodies. This assumption is fundamentally justified by their significant stiffness

difference: the Young's modulus of paddy (375 MPa) is approximately 46.9 times that of rubber (8 MPa). According to Hertz Contact Theory, the calculated equivalent elastic modulus is approximately 10.4 MPa. This value is very close to and slightly higher than the modulus of the rubber itself, indicating that the contact mechanical response is predominantly governed by the rubber, with minimal deformation occurring in the paddy grains, whose mechanical behavior thus approaches that of a rigid body. Therefore, this assumption is mechanically reasonable. It substantially improves computational efficiency while ensuring that the force transmission during contact adheres to the underlying physical principles, although it may slightly overestimate energy transfer during collisions and cannot account for grain breakage. The expression for the equivalent modulus of elasticity E^* is

$$\frac{1}{E^*} = \frac{1-v_1^2}{E_1} + \frac{1-v_2^2}{E_2} \qquad (1)$$

where, E_1, E_2 are the Young's modulus of paddy and rubber, MPa, respectively; v_1, v_2 are the Poisson's ratios of paddy and rubber, respectively[23,24].

3) It is assumed that all paddy grains share identical shape and size. This simplification eliminates the randomness inherent in real grains, which may reduce the model's ability to capture minor stochastic effects such as slight agitation or deflection. However, it provides a clear and controllable starting point for establishing a reproducible baseline model, facilitating the subsequent incorporation of more complex practical factors.

These assumptions strike a balance among computational efficiency, mechanistic clarity, and research objectives. While they may render quantitative results somewhat idealized, they effectively support the qualitative revelation of the core mechanism—that uneven paddy flow leads to uneven wear.

2.2 Finite element model of the interaction between paddy grains and rubber rollers

The single paddy grain physical model is shown in Figure 1a, with a length L_1 of 8.7 mm, a width W_1 of 2.6 mm, a thickness T_1 of 2.0 mm, and an arc radius R_1 of 7.93 mm[25]. In order to simulate the stacked state of paddy grains, a paddy grain cluster physical model is constructed, with a length L_2 of 8.7 mm, a width W_2 of 3.6 mm, and a thickness T_2 of 4.0 mm, as shown in Figure 1b. The diameter of the rubber roller physical model is 78 mm, the thickness of the rubber layer is 5 mm, the axial length is 25 mm, and the hardness of the rubber is Shore A 45-60[23,24].

a. Single paddy grain model

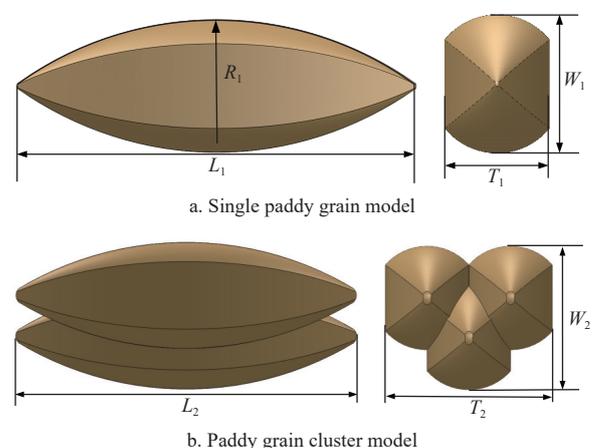

b. Paddy grain cluster model

Figure 1   Single and cluster models of paddy grain

When meshing the rubber roller, the rubber part is divided into 3D hexahedral elements, with different mesh size strategies applied

according to the stress distribution. The part of the rubber roller that comes into contact with paddy grains is the main stress-bearing region, which is meshed with a fine mesh with a size of of 0.4 mm to accurately capture the key mechanical responses of this region during the interaction between the rubber roller and paddy grains. The part of the rubber roller that does not contact paddy grains is the secondary stress-bearing region, which is meshed with a mesh size of 3.2 mm, aiming to balance calculation accuracy and efficiency. Considering that the iron core mainly functions to support the rubber and has an extremely small stress deformation, it is simplified as a rigid body model. Since the main research focuses on the stress response of the rubber part of the rubber roller, the paddy grains and their clusters are also simplified into rigid body models. Based on the geometric dimensions of both, and taking into account the efficiency of simulation calculation, the iron core is divided into a 4 mm tetrahedral mesh, and the paddy grains are divided into a 0.1 mm tetrahedral mesh. The finite element models of the paddy grains and rubber roller are illustrated in Figure 2.

Based on the finite element model described above, a contact mechanics model of paddy grains under uneven feeding states,
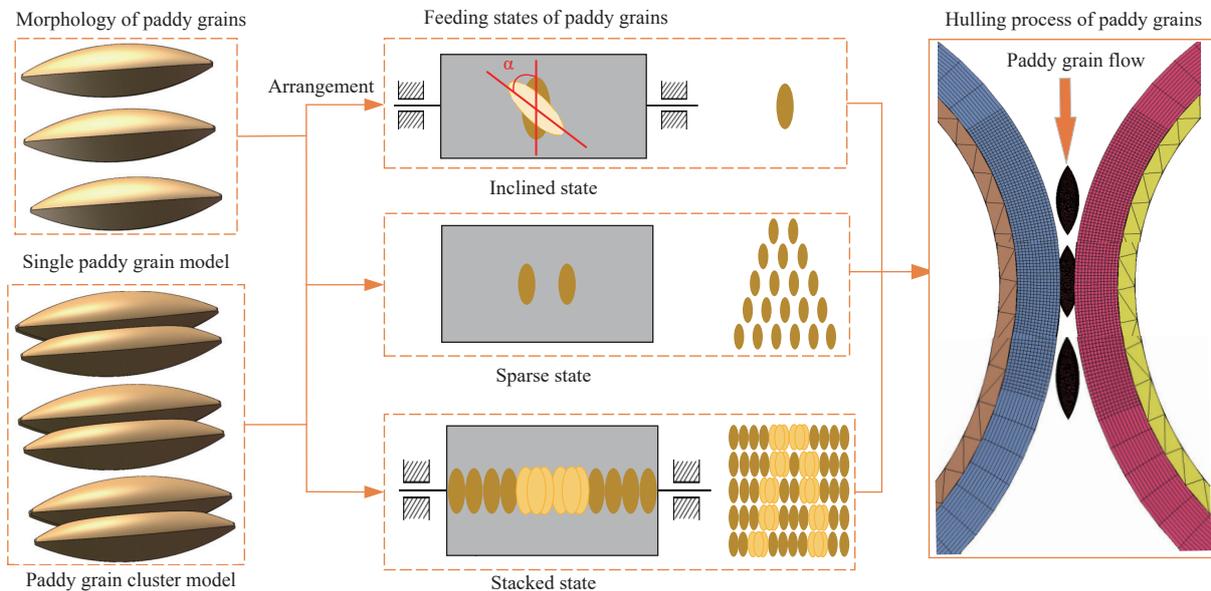
including inclined state, sparse state, and stacked state, is established. This model simulates the entire process of paddy grains being arranged on the surface of the rubber roller and passing through the rolling zone, thereby revealing the mechanism of interaction between the stress state of the rubber roller and its uneven wear. The specific numerical simulation scheme is illustrated in Figure 3.
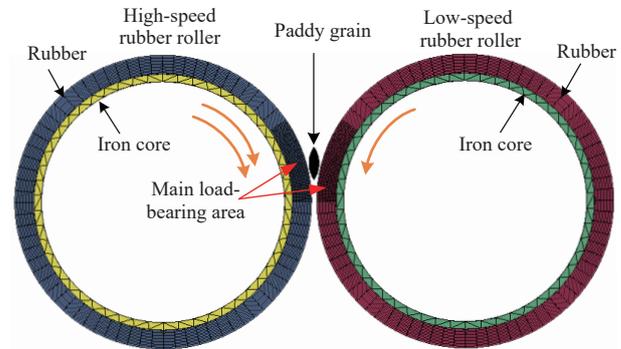

Figure 2   Finite element model of the interaction between paddy grains and rubber rollers

Figure 3   Numerical simulation scheme of the different feeding states of paddy grains

2.3   Contact settings and boundary conditions

Force transmission between rubber rollers and paddy grains is mainly achieved through friction. Therefore, the AUTOMATIC_SURFACE_TO_SURFACE contact model is selected[26]. This model can automatically determine the direction of the contact surface of elements and is stable and accurate when calculating contact forces. For this purpose, it is necessary to establish contact pairs between paddy grains and the rubber of the fast roller, as well as between paddy grains and the rubber of the slow roller, respectively.

To prevent negative volume in calculations and model penetration, the AUTOMATIC_SINGLE_SURFACE self-contact model is added for the rubber. The friction state in this model is dry and unlubricated. The boundary conditions mainly include the following three parts:

1) Set the speed of rubber rollers. To simulate actual hulling conditions, first, a common node constraint is established between the iron core and the rubber fitting surface to ensure that the two move synchronously. Then, parameters for the rubber roller speed are set: the fast rubber roller has a linear speed of 14.8 m/s, and the

linear speed difference between the fast and slow rubber rollers is 2.3 m/s.

2) Apply a transverse dynamic load to the paddy grains. During normal hulling, paddy grains enter the nip zone of the rubber rollers via the flow plate under their own weight. If the rubber rollers are too hard or the roller gap is too small, paddy grains may fail to pass through the nip zone smoothly, which will cause simulation failure. Therefore, a dynamic load of 0.1 N is applied along the longitudinal axis of the paddy grains to ensure their smooth passage through the nip zone of the rubber rollers.

3) Add constraints. After applying the dynamic load to the paddy grains, displacement constraints should also be applied to them in the direction perpendicular to their long axis to ensure no displacement occurs perpendicular to the motion plane. Meanwhile, the rubber roller core should be constrained in the X, Y, and Z directions to ensure stability during the simulation.

2.4   Material parameters

When constructing the finite element model of the rubber roller-paddy grain system, the 001-ELASTIC material model is adopted for the rubber layer of the rubber roller. This model is based on the

classic Hooke's Law and is a linear elastic material model suitable for describing the stress-strain relationship of isotropic materials within the range of small deformations. For the paddy grains and the iron core, the 020-RIGID material model is adopted. This model falls into the category of rigid body material models and is mainly used to simulate the mechanical response characteristics of idealized rigid objects. During stress application, the object does not undergo any deformation, making it suitable for scenarios where high computational efficiency is required and the impact of deformation is negligible. The physical parameters of the material models for the paddy grains, rubber layer, and iron core are presented in Table 1[23-25]. The actual performance of rubber varies with its composition, processing, and service conditions. In this study, a set of fixed parameters is adopted to establish a baseline analytical model, aiming to reveal the mechanical mechanisms and primary influencing factors of wear.

Table 1   Main parameters of the finite element model

Types	Parameters	Values
Paddy grain	Density ρ_1/kg·m^{-3}	1350
	Poisson's ratio v_1	0.25
	Young's modulus E_1/Mpa	375
Rubber layer	Density ρ_2/kg·m^{-3}	1200
	Poisson's ratio v_2	0.5
	Young's modulus E_2/Mpa	8
Iron core	Density ρ_3/kg·m^{-3}	7830
	Poisson's ratio v_3	0.29
	Young's modulus E_3/Mpa	2.07×10^5
Paddy-rubber	Coefficient of static friction μ_s	0.5
	Coefficient of rolling friction μ_k	0.01

2.5 Evaluation indicators for rubber roller wear

To ensure the comparability of numerical simulation results, uniform simulation parameters are adopted for various feeding states, and the maximum contact pressure, maximum von Mises stress, and the time difference between their peaks are selected as evaluation indicators for rubber roller wear. Among them, the maximum contact pressure refers to the maximum extrusion stress perpendicular to the long axis direction of paddy grains that the rubber roller bears after the paddy grains enter the rolling zone, characterizing the extrusion strength. This study directly reveals the key locations and initiation mechanisms of wear through the aforementioned indicators. The distribution of von Mises stress is directly related to the distortion energy density within the material, and the identified high-stress regions essentially correspond to the core areas where plastic deformation energy accumulates and dissipates, thereby providing a positional basis for energy analysis at the mechanical level. The current work primarily aims to establish a qualitative discrimination framework for wear risk; therefore, quantitative integration of energy dissipation has not been performed.

This section aims to establish a mechanical framework for the qualitative analysis of roller wear risk. The derivation is based on the following core assumptions:

1) The contact between paddy and the rubber roller conforms to the Hertz Contact Theory for isotropic, linearly elastic materials.

2) The contact is simplified as an elliptical point contact model. The purpose of the theoretical derivation is to reveal the intrinsic mechanistic relationship between von Mises stress and the fundamental physical quantities of contact. According to Hertz Contact Theory, when the contact between paddy and the rubber roller is an elliptical point contact, the maximum contact pressure is

$$P_{max} = \frac{3F}{2\pi ab} \tag{2}$$

where, F is the normal load, N; a and b are the semi-major and semi-minor axes of the contact ellipse, mm, respectively, i.e., its major axis $2a$ is equal to the geometric major axis L_1 of the paddy grain, and the minor axis $2b$ matches the geometric minor axis W_1 of the grain.

To evaluate the stress state at any point within the contact zone, the complete stress tensor at that point must be obtained. According to Hertz Contact Theory, the stress state at any point (x, y, z) inside the contact zone can be fully determined by the maximum contact pressure P_{max} and the geometry of the contact ellipse (a, b). That is, each stress component can be expressed in the following form:

$$\sigma_x, \sigma_y, \sigma_z, \tau_{xy}, \tau_{yz}, \tau_{zx} = f_i(P_{max}, a, b, x, y, z), \ i \in \{x, y, z, xy, yz, zx\} \tag{3}$$

Where, σ_x, σ_y, σ_z denotes the normal stress, MPa; τ_{xy}, τ_{yz}, τ_{zx} denotes the shear stress, MPa; and f_i indicates that the specific functional form is determined by the theory of elasticity.

To extract a scalar indicator from the complex stress state for evaluating the risk of plastic yielding in materials, the von Mises stress is introduced. It can be used to analyze the impact of squeezing and shearing effects during husking on the strength and safety of rubber rolls. According to elastoplastic mechanics, the von Mises stress σ_{vm} can be defined by the second invariant of the deviatoric stress tensor J_2, whose expression is

$$\sigma_{vm} = \sqrt{3J_2} \tag{4}$$

If the six independent components of the total stress tensor (normal stresses σ_x, σ_y, σ_z; shear stresses τ_{xy}, τ_{yz}, τ_{zx}) are known, the expression of J_2 based on the "original Cartesian coordinate system" is

$$J_2 = \frac{1}{6} \left[(\sigma_x - \sigma_y)^2 + (\sigma_y - \sigma_z)^2 + (\sigma_z - \sigma_x)^2 + 6(\tau_{xy}^2 + \tau_{yz}^2 + \tau_{zx}^2) \right] \tag{5}$$

Substituting Equation (5) into (4), the expression of von Mises stress in three-dimensional space can be obtained:

$$\sigma_{vm} = \sqrt{\frac{1}{2}[(\sigma_x - \sigma_y)^2 + (\sigma_y - \sigma_z)^2 + (\sigma_z - \sigma_x)^2 + 6(\tau_{xy}^2 + \tau_{yz}^2 + \tau_{zx}^2)]} \tag{6}$$

According to Equation (6), when the shear stress components are larger or the difference between normal stress components is larger, the von Mises stress is also larger, and the possibility of plastic yielding of rubber materials is greater, so the rubber roller is more likely to wear. The von Mises stress and contact pressure are indirectly correlated through the "distribution of normal stress components" and the "contribution of shear stress".

The time difference between the maximum values of contact pressure and von Mises stress reflects the dynamic stability of the interaction system between the rubber roller and paddy grains during operation. Let t_{vm} be the peak time when the von Mises stress reaches its maximum value, and t_p be the peak time when the contact pressure reaches its maximum value, then the peak time difference between them is

$$\Delta t = t_p - t_{vm} \tag{7}$$

If Δt is very small or close to zero, it indicates that the maximum values of contact pressure and von Mises stress occur almost simultaneously, and the dynamic load transfer of the system is synchronous. At this time, the rubber roller will bear the maximum extrusion force and the maximum equivalent stress causing plastic deformation at the same moment, leading to

accelerated wear or even failure of the rubber roller. If $\Delta t \neq 0$, the two maximum values do not occur simultaneously, and there is a "buffer" in the dynamic load transfer of the system. When $\Delta t > 0$, the maximum contact pressure appears first. After the rubber roller bears the maximum extrusion force, its internal stress accumulates and redistributes. It then reaches the maximum equivalent stress that causes plastic deformation. Extrusion acts as the initial driving factor, and subsequent stress concentration triggers wear. When $\Delta t < 0$, the maximum von Mises stress appears first. This indicates that the internal stress concentration of the rubber reaches the critical state for plastic deformation before the contact pressure reaches its maximum. This may be related to factors such as the surface texture of the rubber roller, the shape of paddy grains, or uneven internal stress of the material. This situation may cause local premature wear of the rubber roller.

3   Numerical results and analysis

3.1   Effect of inclined paddy grain on the contact mechanical properties of rubber rollers

To investigate the effect of inclined distribution of paddy grains on the contact mechanical properties of rubber rollers, the mechanical responses of the rubber rollers under different orientation angles were obtained via numerical simulation under the conditions of a fixed rolling spacing of 1.6 mm and a single paddy grain. As shown in Figure 4, the proportion of the hourglass energy to the total internal energy is less than 5%, which indicates that the hourglass mode control is effective, providing a basis for validating the reliability of this set of simulation data[27].
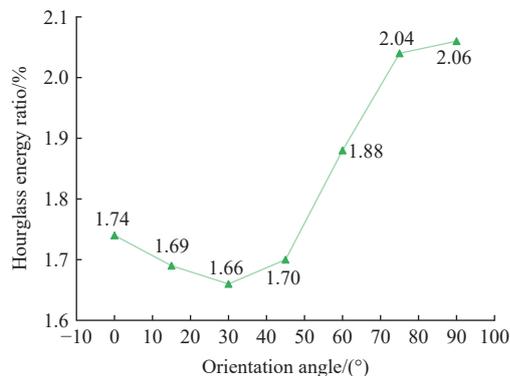

Figure 4   Hourglass energy ratio under different orientation angles

3.1.1   Variation law of maximum contact pressure

As shown in Figure 5, when the orientation angle varies from 0° to 30°, the maximum contact pressure on the rubber roller surface increases from 5.99 MPa to 12.63 MPa, with an increase rate of 111%. This is attributed to the reduced instantaneous contact area caused by the inclination of the grains, which leads to a sharp surge in the load per unit area.

When the orientation angle exceeds 30°, the contact pressure drops to 3.12 MPa, a decrease of 75%, due to the interruption of load transmission caused by contact instability. As illustrated in Figure 6a, this phenomenon is specifically manifested as the disruption of the contact region caused by the slippage of paddy grains[28]. Within the range of 45° to 90°, the maximum contact pressure stabilizes at approximately 2.55 MPa. This is because the instantaneous elliptical contact area between the paddy grains and the rubber roller surface is relatively large, which makes the contact pressure distribution more uniform, enhances the load dispersion effect, and thus maintains the contact pressure at a low level, as shown in Figure 6b.
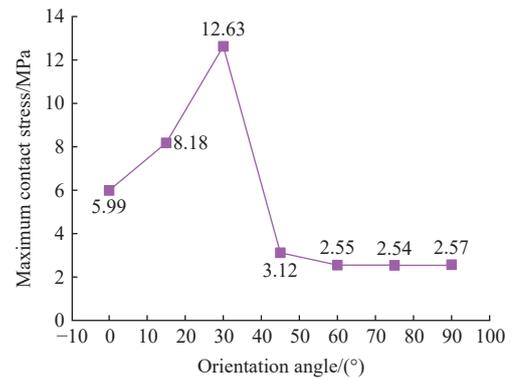

Figure 5   Maximum contact pressure of rubber rollers under different orientation angles
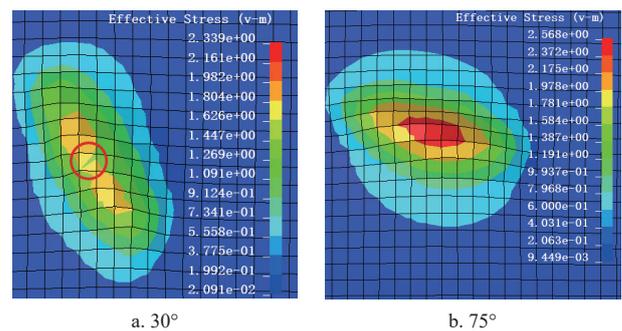

a. 30°   b. 75°

Figure 6   Effect of typical paddy grain orientation angles on von Mises stress of rubber rollers

3.1.2   Evolution characteristics of maximum von Mises stress

According to Figure 6 and Figure 7, in the orientation range of 0° to 30°, the maximum contact pressure increases from 5.99 MPa to 12.63 MPa, while the von Mises stress only decreases slightly from 2.45 MPa to 2.34 MPa. The von Mises stress shows a positive correlation with the normal contact pressure, a trend resulting from the weakening of lateral constraint stress caused by paddy grain inclination, but the stress state is still dominated by the normal component.
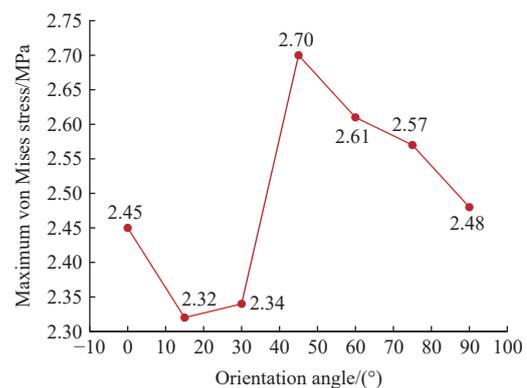

Figure 7   Maximum von Mises stress of rubber rollers under different orientation angles

The increased contact pressure at this stage directly raises the risk of overloading the rubber rollers in the normal direction. At 45°, the contact pressure drops to a minimum of 3.12 MPa, but the von Mises stress rises to a peak of 2.70 MPa, 15.4% higher than that at 30°. This indicates that shear is dominant at this stage: the von Mises stress is determined by the shear stress term (decoupled from the normal force), and an increase in contact pressure does not necessarily increase the von Mises stress, but shear distortion exacerbates the fatigue damage of the rolls. When the angle exceeds

60°, the von Mises stress decreases as the contact area increases, from 2.61 MPa to 2.48 MPa, and the stress tends to be uniformly distributed.

3.1.3 Dynamic characteristics of time difference

According to Figure 8, when the orientation angle is in the range of 0° to 45° or is 75°, Δt is very small or close to zero. This indicates that the peaks of contact pressure and von Mises stress appear almost simultaneously and that the system's dynamic loads are transmitted synchronously. In this case, the rubber roller bears both the maximum extrusion force and the maximum equivalent stress, causing plastic deformation and making it prone to accelerated wear or even failure. When the orientation angle is 60° or 90°, Δt=0.2 ms, meaning that the peak contact pressure appears first. After the rubber roller bears the maximum extrusion force, the internal stress accumulates and redistributes before reaching the maximum equivalent stress that causes plastic deformation, and extrusion is the initial driving factor. The coupling effect of the shear stress generated by the violent slipping of the paddy grains, together with the lag in the shear deformation response caused by the viscoelasticity of the rubber behind the loading of the normal contact force, forms a "buffer" effect, which is essentially consistent with the mechanism of "the lag effect originating from the elastic creep of materials", as revealed by Huang[29]. Meanwhile, the dynamic friction and thermal effects generated by slipping accelerate the wear of the rubber roller, and elastic creep also causes cumulative damage through the lag effect.
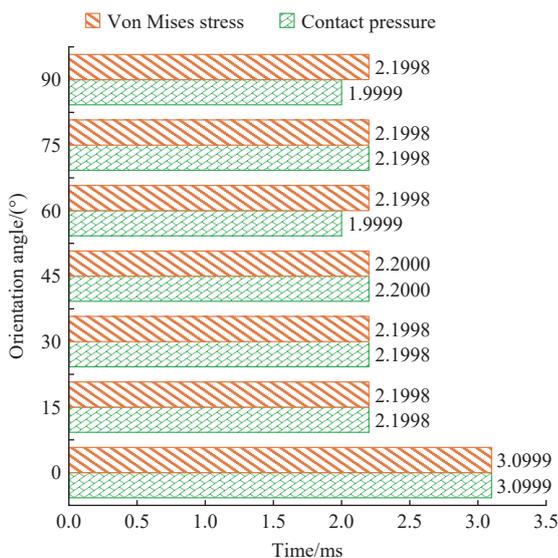

Figure 8   Peak times of maximum contact pressure and maximum von Mises stress under different orientation angles

3.1.4 Risk discussion of rubber roller wear

When the paddy orientation angles are at 0° and 15°, both the contact pressure and von Mises stress remain at moderate levels, leading to a low risk of uneven wear of the rubber rollers. When the orientation angle increases to 30°, the peak contact pressure increases by approximately 111% compared to the 0° condition, which facilitates the rice husk cracking but elevates the wear risk of the rubber rollers. Under the 45° condition, the shear stress becomes dominant, which is prone to causing distortion of the stress field on the roller surface and exacerbating uneven axial wear of the rubber rollers. Under the large-angle conditions of 60° to 90°, although the contact pressure is more stable and the wear rate decreases, the normal contact pressure decays below the critical hulling threshold, which affects the hulling rate.

In the paddy hulling process, the maximum contact pressure is positively correlated with the hulling rate. Under the 30° condition, the structure of the paddy husk is effectively destroyed by normal extrusion, and the theoretical hulling rate is the highest, but the crushing rate and the wear rate of the rubber rollers will increase. Under the 45° condition, the theoretical hulling rate is lower than that at 30°. Additionally, the shear stress dominates, and the uneven wear of the rubber rollers increases. Compared with the condition of 30°, the contact pressures at 0° and 15° are lower, the hulling efficiency is moderate, and the stress is not overloaded, making the overall efficiency optimal. Under the operating conditions of 60° to 90°, the contact pressure stabilizes at approximately 2.5 MPa, and at this point, the theoretical hulling rate is the lowest. However, the contact area is the largest, and the wear of the rubber rollers is less severe. Nevertheless, the relatively low contact pressure of the rubber rollers will reduce the hulling performance of the huller. Chen et al.[9] pointed out that a paddy orientation angle of 0° is most favorable for paddy hulling, and the hulling rate decreases linearly with an increase in the orientation angle, a finding that is in good agreement with the results of the present numerical calculation.

3.2 Effect of sparse paddy grain on the contact mechanical properties of rubber rollers

In order to investigate the effect of the sparse distribution of paddy grains on the contact mechanical properties of the rubber rollers, the roller gap of the two rubber rollers was fixed at 1.6 mm, the orientation angle of the paddy was 0°, and the number of grains was varied from 2 to 6 for the simulation.

3.2.1 Variation law of maximum contact pressure

Figure 9 presents the maximum contact pressure for the sparse arrangement of different numbers of paddy grains. When the number of paddy grains increases from 2 to 3, the maximum contact pressure rises from 5.70 MPa to 6.56 MPa, an increase of 15.1%. At this point, the contact pressure concentration in the roller area corresponding to the middle grains arises because these grains are constrained by the grains on both sides, forming bidirectional extrusion. That is, the contact pressure fields of neighboring grains interfere with each other, resulting in a higher normal load than that of the edge grains, whereas the end grains have a much lower contact stress level due to the large grain spacing and load dissipation. When the number of grains increases to 4, the maximum contact pressure falls back to 6.20 MPa, a decrease of 5.5%. The symmetrical distribution of paddy grains causes the load of the middle grains to be transferred to the roller ends, mitigating the contact pressure concentration in the middle of the rubber roller. When the number of grains is 5, the maximum contact pressure increases to 7.09 MPa, representing an increase of 14.3% compared
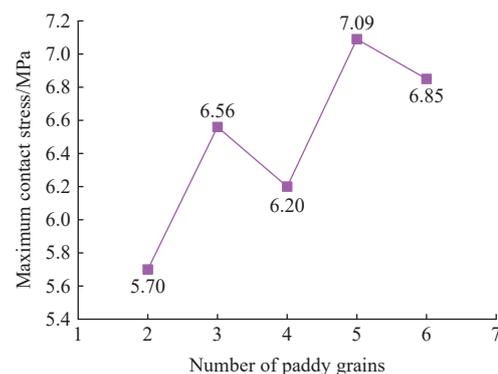

Figure 9   Maximum contact pressure of rubber rollers under different numbers of paddy grains

with the 4-grain case. The odd number of grains breaks the balance of "symmetric load shunting", so the load cannot be completely dispersed to both ends, forcing the middle region to bear a higher normal load. When the number of grains increases to 6, the maximum contact pressure decreases to 6.85 MPa, a decrease of 3.4% compared with the 5-grain case. An increased grain count thus effectively redistributes the pressure at the roller ends.

3.2.2   Evolution characteristics of maximum von Mises stress

As shown in Table 2, when the number of grains varies from 2 to 6, the maximum von Mises stress rises from 2.51 MPa to 2.74 MPa, representing an overall increase of 9.2%. Combined with Equations (2), (4), and (5), it can be seen that when the number of grains is 3 or 4, the maximum von Mises stress is greater than the corresponding contact pressure, which indicates that shear stress dominates. When the number of grains is 3, the end grains are constrained by the edge of the rollers, resulting in limited slip, as shown in Figure 10a. The stress distribution of the fast and slow rubber rollers is uneven, giving rise to stress concentration. When

a. With 3 paddy grains

b. With 4 paddy grains

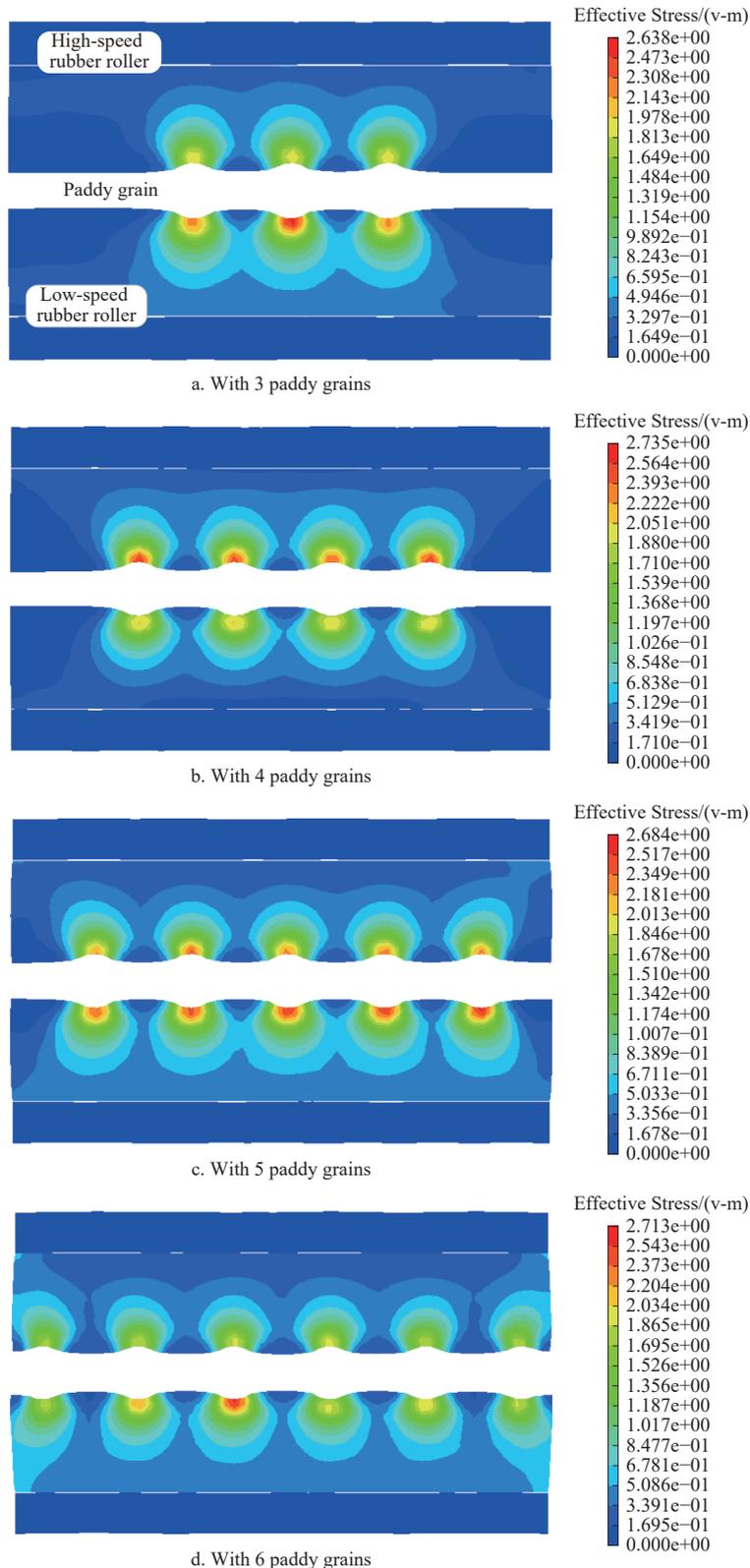c. With 5 paddy grains

d. With 6 paddy grains

Figure 10   Stress distribution contour on rubber roller cross-section under different numbers of paddy grains

the number of grains is 4, the superposition of grain shear stresses causes the maximum von Mises stress to rise by 9.2%, as shown in Figure 10b and Figure 11, which reflects the variation in the von Mises stress of the rubber rollers induced by shear forces.

Table 2   Maximum von Mises stress and corresponding contact pressure under different numbers of paddy grains

Total number of grains	Maximum von Mises stress/MPa	Stress peak time/ms	Contact pressure/MPa
2	2.51	2.6000	2.55
3	2.64	3.1999	2.48
4	2.74	2.9999	2.64
5	2.68	3.9999	5.05
6	2.71	4.0000	3.31

When the number of grains is 5, the stress falls back to 2.68 MPa, a 2.2% decrease, as shown in Figure 10c. This indicates that the increase in normal contact pressure does not synchronously enhance the contribution of shear deformation, and the non-uniformity of the stress distribution on the rubber rollers has been moderated to some extent by the odd-numbered distribution. Additionally, the risk of the material undergoing plastic yielding is reduced, but attention needs to be paid to the hulling uniformity of edge paddy grains.

When the number of grains is 6, the stress rises slightly to 2.71 MPa, as shown in Figure 10d. The symmetrical distribution of 6 paddy grains makes the stress distribution of the rollers exhibit the characteristics of "concentrated in the middle and dispersed at both ends", and the overall stress uniformity is still superior to that of 5 paddy grains (an odd number). The primary root of the stress rise is that the contact density of 6 paddy grains increases, and the spacing between grains decreases, resulting in the interference and superposition of stress fields of adjacent grains. Furthermore, the normal load and tangential slip of intermediate grains act in conjunction to enhance the contribution of shear deformation energy, a core component of von Mises stress, which ultimately drives the von Mises stress to recover slightly.
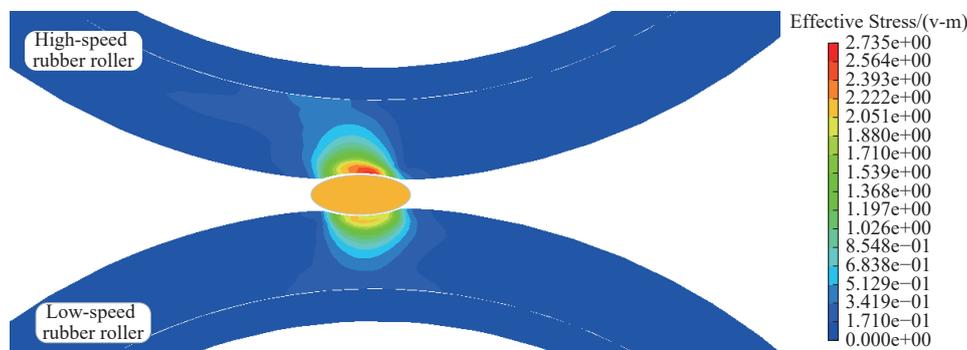

Figure 11   Sectional stress cloud diagram of rubber roller at outermost grain position with 4 paddy grains

3.2.3   Dynamic characteristics of peak time difference

As shown in Figure 12, when the number of paddy grains is 2, 3, 4, or 6, the maximum contact pressure occurs later than the maximum von Mises stress; when the number of paddy grains is 5, the maximum contact pressure occurs earlier than the maximum von Mises stress. When the number of paddy grains is 2 or 3, the time difference between the stress peaks remains stable at 1.0 ms. Due to the different curvatures of the edge and middle parts of the rubber roller, the edge grains experience weaker extrusion constraints and slower tangential sliding. The contact pressure relies on the rolling of the rubber roller to supplement the applied load, whereas by contrast, the von Mises stress peaks earlier because middle grains first form a shear-normal coupling effect.

When the number of paddy grains is 4, the paddy grains are arranged in a completely symmetrical and uniform manner, and the time difference decreases to 0.1999 ms. This symmetrical and uniform distribution enables uniform transmission of the extrusion load, ensuring the middle grains bear balanced loads. After reaching the maximum extrusion stage, the middle grains unload quickly to release excess contact pressure. Furthermore, the peak contact pressure emerges earlier due to the uniform load transmission, reducing the peak time difference relative to the von Mises stress. When the number of paddy grains is 5, the asymmetrical distribution leads to weak unilateral constraints on the end grains. The viscoelastic hysteresis of the rubber roller slows down the rise in shear stress, increasing the time difference to 0.8 ms. When the number of paddy grains is 6, although the grains are arranged symmetrically, the high contact density and superposition of stress fields cause dynamic fluctuations, resulting in a deviation in peak synchronization. The time difference also stabilizes at approximately 0.6 ms.
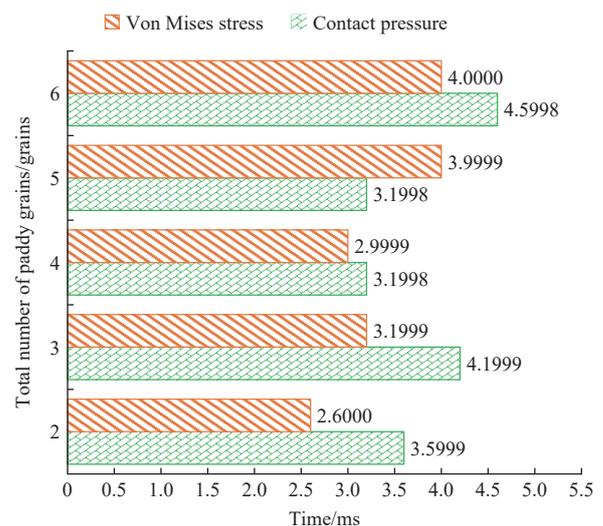

Figure 12   Peak times of maximum contact pressure and maximum von Mises stress under different numbers of paddy grains

3.2.4   Risk discussion of rubber roller wear

As can be seen from the above analysis, when the number of paddy grains is 3, the shear fatigue risk in the middle of the rubber roller is relatively high. When the number of paddy grains is 4, the shear fatigue risk in the rubber roller's middle part is moderate, with the von Mises stress reaching 2.74 MPa at this time. When the number of paddy grains is 5, the contact pressure overload risk in

the rubber roller's middle part is the highest, with the contact pressure peaking at 7.09 MPa. When the number of paddy grains is 6, compared with other grain quantities, the uneven wear risk is the lowest, with the von Mises stress at 2.71 MPa. Since the wear risk of the rubber roller is relatively low when the number of paddy grains is 6, a control group with dense arrangement was established to observe the stress variation of the rubber roller. In accordance with the effective length of the rubber roller, the number of paddy grains is increased to 12. At this time, the two distribution patterns of paddy grains on the rubber roller are shown in Figure 13.

a. With 6 paddy grains
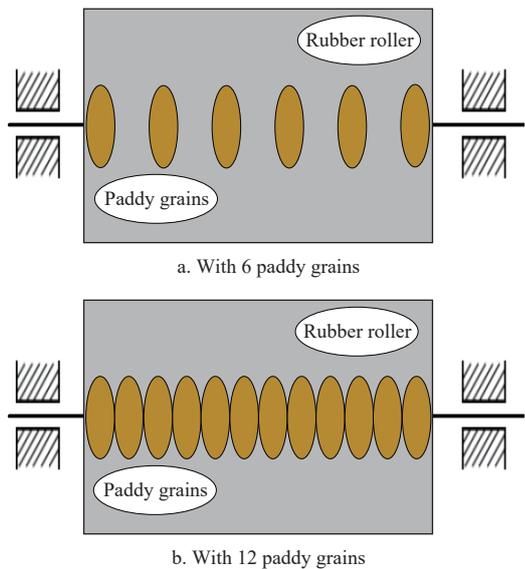

b. With 12 paddy grains

Figure 13   Schematic diagram of paddy grain distribution on rubber rollers with 6 and 12 grains

According to Table 3, the total width of 12 densely arranged paddy grains and 6 paddy grains arranged with a 2.5 mm spacing is basically the same, with a difference rate of 2.04%. In terms of the maximum contact pressure and the maximum von Mises stress, the values of these two indicators are nearly identical, with difference rates of 1.02% and 3.32% respectively, indicating that the grain quantity and distribution interval have little impact on these two stress indicators. The maximum von Mises stresses under the two working conditions are nearly equal, indicating that shear slip is still the primary cause of rubber roller damage.

Table 3   Comparison of contact mechanical properties of rubber rollers with 12 densely and 6 sparsely arranged paddy grains

Parameter	Dense distribution/ 12 grains	Sparse distribution/ 6 grains	Result comparison
Total width/mm	24.0	24.5	Basically the same, with a difference rate of 2.04%
Maximum contact pressure/MPa	6.92	6.85	Basically equal, with a difference rate of 1.02%
Maximum von Mises stress/MPa	2.80	2.71	Basically equal, with a difference rate of 3.32%
Peak time difference/ms	0.20	0.60	More synchronous dynamic response with 12 grains

In terms of time difference, the time difference for 12 densely arranged grains is 0.20 ms, and that for 6 sparsely arranged grains is 0.60 ms. This shows that when the paddy grains are sparsely arranged, the operational stability of the rubber roller is poor, and the wear risk is high, which is not suitable for high-efficiency continuous production; while when densely arranged, the

synchronization between the contact pressure and the von Mises stress is high, the operational stability of the rubber roller is improved, and the wear risk is low, making it suitable for high-speed continuous production.

3.3   Effect of stacked paddy grains on the contact mechanical properties of rubber rollers

As shown in Figure 3, in order to simulate the stacked paddy grains, grain clusters are introduced into the paddy grain flow while ensuring that the surfaces of the rubber rollers are fully covered with grains. During the simulation, the number of grain clusters and the roller gap of the rubber rollers are kept constant, and the influence of grain clusters on the contact mechanical properties of the rubber rollers is investigated by changing the spacing between them.

3.3.1   Variation law of maximum contact pressure

As shown in Figure 14, when the spacing between grain clusters increases from 0 mm to 2 mm, the contact pressure rises from 10.06 MPa to 13.85 MPa, with an increase rate of 37.7%. This is because the ultra-local high-stiffness zone formed when grain clusters are adjacent causes pressure concentration, as illustrated in Figure 15a. In the range from 2 mm to 6 mm, the contact pressure fluctuates stably between 13.5 MPa and 13.7 MPa. At this stage, the filling grains between the two adjacent clusters disperse part of the load, but the presence of the clusters still leads to high-level fluctuations in contact pressure. When the spacing increases to 8 mm, the pressure drops to 13.17 MPa. At this point, the filling grains further balance the von Mises stress on the rubber roller, though the rubber at the grain clusters still bears a slight concentrated load, as shown in Figure 15b.
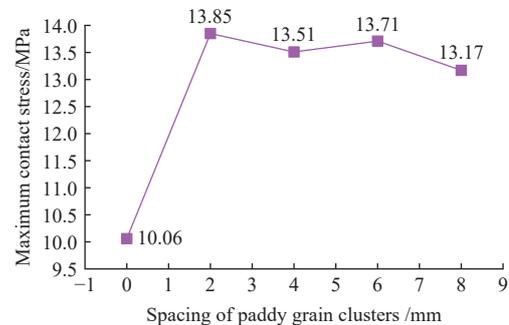

Figure 14   Maximum contact pressure of rubber rollers under different spacings between grain clusters

3.3.2   Evolution characteristics of maximum von Mises stress

As shown in Figure 16, with the increase in the spacing of paddy grain clusters, the maximum von Mises stress shows a trend of first decreasing slowly, then dropping rapidly to the lowest point, and finally rising significantly. When the paddy grain cluster spacing ranges from 0 to 6 mm, the von Mises stress decreases from 5.44 MPa to 5.18 MPa, with a reduction of 4.8%.

When the spacing between paddy grain clusters is small, the grains are in dense contact with the rubber rollers. This creates a weak superposition effect in the contact pressure fields of adjacent grains, making the normal stress distribution more uniform and slightly reducing the shear stress. This, in turn, leads to a small decrease in von Mises stress. As the spacing increases further, the grain clusters become more scattered and the superposition effect of the contact stress fields weakens significantly. The grains are almost in isolated contact with the rubber rollers, resulting in a significant reduction in the normal stress difference and a significant decrease in shear stress. This causes von Mises stress to drop rapidly.

a. 2 mm spacing of paddy grain clusters

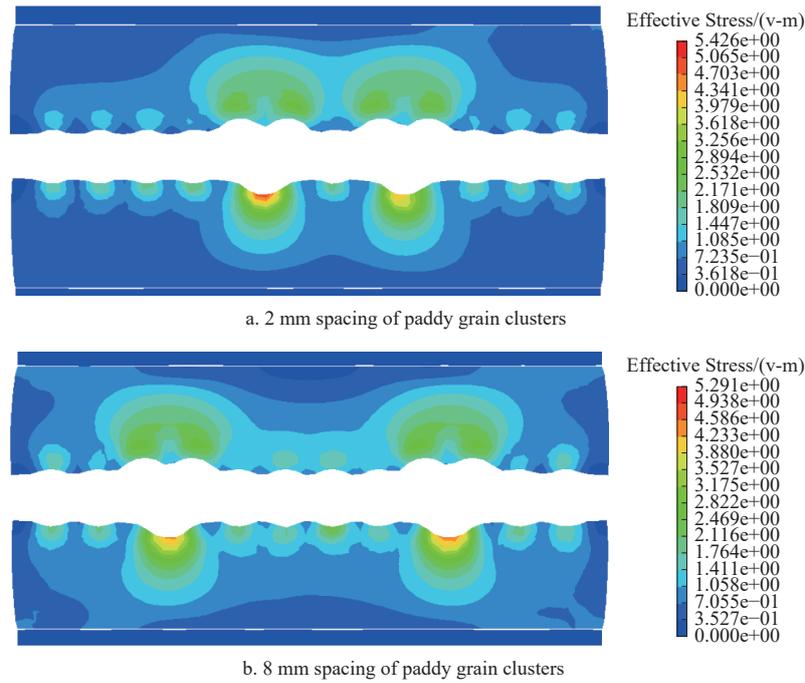b. 8 mm spacing of paddy grain clusters

Figure 15　Sectional stress cloud diagrams of rubber rollers for grain clusters under different spacings
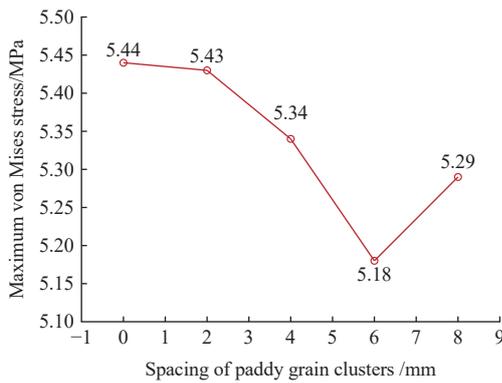

Figure 16　Effect of paddy grain clusters on the maximum von Mises stress of rubber rollers

However, when the spacing further increases from 6 mm to 8 mm, the von Mises stress rises again from 5.18 MPa to 5.29 MPa,

with an increase of 2.1%. This is because the grain clusters are excessively scattered, which changes the transmission path of contact loads. Contact pressure is more concentrated on a small number of grains, leading to a re-increase in the local normal stress difference and a corresponding rise in shear stress—hence the subsequent increase in von Mises stress. In addition, as shown in Figure 17, the slip of grains at the end of the rubber rollers is restricted, causing local shear stress concentration.

3.3.3　Dynamic characteristics of time difference

As shown in Figure 18, when the grain cluster spacing is 0 mm, the time difference (Δt) is 1.0000 ms ($\Delta t>0$). The maximum contact pressure occurs when the rubber rollers bear the maximum extrusion force. The internal stress of the rubber rollers then accumulates and redistributes before reaching the maximum equivalent stress that causes plastic deformation. However, due to the presence of a "buffer" effect, the wear rate is relatively controllable.
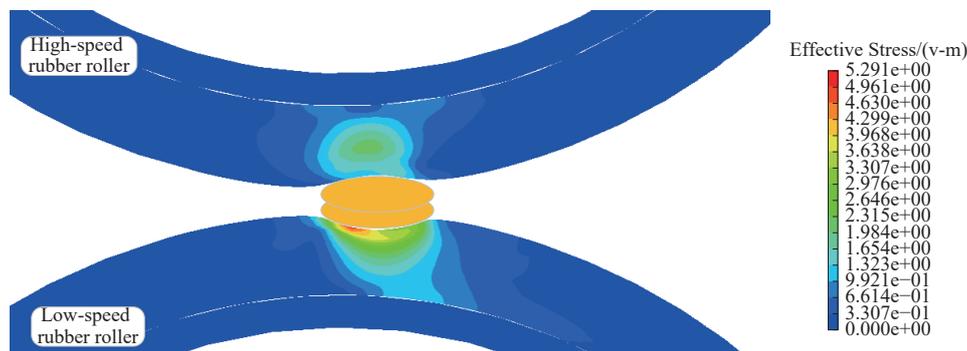

Figure 17　Sectional stress cloud diagram of rubber rollers for paddy grain clusters with an 8 mm spacing

When the spacing is 2 mm or 8 mm, $\Delta t=0$. The maximum values of contact pressure and von Mises stress occur almost simultaneously, and the system transmits dynamic loads synchronously. At this point, the rubber rollers bear both the maximum extrusion force and the maximum equivalent stress that causes plastic deformation. Without a "buffer" effect, wear would accelerate or the system could fail.

When the spacing is 4 mm or 6 mm, $\Delta t>0$ and decreases

gradually. The maximum contact pressure appears first, and with a "buffer" effect, the internal stress of the rubber rollers can accumulate and redistribute. However, as the spacing increases, Δt decreases, reducing the "buffer" effect and increasing the wear risk. Even so, the risk remains lower than that when Δt is 0.

3.3.4　Risk discussion of rubber roller wear

When the spacing between grain clusters is 0 mm, the rubber rollers are at relatively high risk of shear fatigue and hysteresis

damage. Although the contact pressure is concentrated due to the ultra-local high-stiffness zone and the time difference (Δt>0) provides a "buffer" effect, the maximum von Mises stress remains high. Consequently, the rubber rollers still face a certain degree of wear risk (with a relatively controllable rate) and accelerated surface crack initiation.
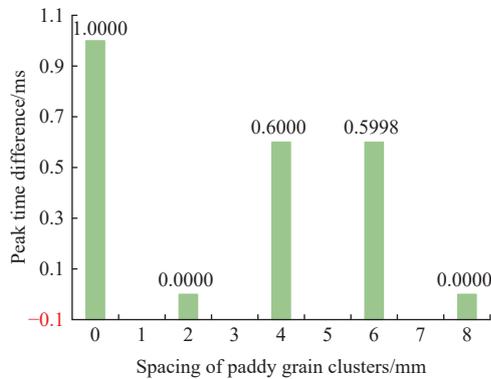

Figure 18   Peak time difference between contact pressure and von Mises stress under different spacing of paddy grain clusters

At a spacing of 2 mm, the contact pressure reaches its maximum value of 13.85 MPa, which leads to the highest risk of surface stress overload for the rubber rollers. Additionally, the peaks of contact pressure and von Mises stress occur simultaneously (Δt=0), leaving the system without a "buffer" effect. The rubber rollers therefore experience both the maximum extrusion force and the maximum equivalent stress, which induce plastic deformation simultaneously, significantly increasing the risk of wear and easily inducing local plastic deformation or even accelerated failure.

When the spacing is 4 mm or 6 mm, however, a "buffer" effect exists (Δt>0), which allows the internal stress of the rubber rollers to accumulate and redistribute. Consequently, the wear risk is lower than that when Δt is 0. Specifically, at a spacing of 6 mm, the maximum von Mises stress drops to 5.18 MPa, the minimum value, and the shear components are evenly distributed. This results in the lowest risk of plastic yielding and uneven wear for the rubber rollers. However, as the spacing increases from 4 mm to 6 mm, Δt decreases, the "buffer" effect weakens, and there is a slight upward trend in wear risk.

At a spacing of 8 mm, the peaks of contact pressure and von Mises stress coincide (Δt=0), and there is no "buffer" effect. The rubber rollers bear both the maximum extrusion force and the maximum equivalent stress, which induce plastic deformation and significantly elevate the wear risk. Furthermore, the rubber rollers are subject to a moderate risk of shear stress concentration at the ends, which can easily result in localized spalling.

In summary, when the grain cluster spacing is 6 mm, the surface contact pressure of the rubber rollers is relatively high, but the stress distribution is more uniform. The maximum von Mises stress decreases by 4.8%, and the dynamic response time difference is reduced by 40%, providing the rubber rollers with relatively optimal performance in terms of load-bearing capacity, stress distribution uniformity, and dynamic stability.

Furthermore, according to Table 3, when the number of densely arranged paddy grains is 12, the contact pressure is 6.92 MPa, the maximum von Mises stress is only 2.8 MPa, and the time difference is 0.2 ms. All performance indicators are superior to those of the paddy grain flow with the introduced grain clusters. This indicates that uneven wear of the rubber rollers is inevitable with paddy grain stacking.

4   Conclusions

Abnormal feeding states of paddy grain flows are the key factors leading to the uneven wear of rubber rollers in rice hullers. In this study, the nonlinear finite element simulation model of paddy-rubber roller interaction was established, with the three indicators of maximum contact pressure, the maximum von Mises stress, and the peak time difference between them as evaluation indicators. The effects of abnormal distribution (e.g., paddy grains inclination, sparseness, and stacking) on the contact mechanical properties of rubber rollers were analyzed through simulation, and the conclusions are as follows:

1) When the paddy grain orientation angle is within the range of 0° to 30°, the maximum contact pressure increases from 5.99 MPa to 12.63 MPa, representing an increase of 111%. Meanwhile, the von Mises stress decreases slightly. At 45°, by contrast, the contact pressure drops to 3.12 MPa, and the von Mises stress is 2.70 MPa, with the load dominated by shear stress. At this point, there is no peak time difference and both the rubber roller wear rate and the hulling rate are unsatisfactory. When the angle ranges from 60° to 90°, the contact pressure stabilizes at approximately 2.55 MPa, and a time difference buffering effect exists at some angles, resulting in slight rubber roller wear. At 0° and 15°, however, both contact pressure and von Mises stress are at medium levels, with no peak time difference, and the overall performance regarding hulling efficiency and wear risk is optimal. This is consistent with the results of relevant studies.

2) When the number of paddy grains increases from 2 to 3, the contact pressure rises to 6.56 MPa, an increase of 15.1%; this configuration induces a higher shear fatigue risk in the middle of the rubber rollers. With 4 grains, by contrast, the maximum contact pressure decreases, and the von Mises stress increases to 2.74 MPa, with the load bearing dominated by shear stress. When 5 grains are present, the contact pressure reaches 7.09 MPa, inducing the highest contact pressure overload risk in the middle of the rubber rollers. With 6 grains, the maximum contact pressure drops to 6.85 MPa, yielding the lowest uneven wear risk among sparse distribution conditions. A comparison of the sparse distribution of 6 grains and the dense distribution of 12 grains shows their key contact stress indicators are nearly identical. The dense distribution, however, exhibits a smaller peak time difference, enhanced dynamic operational stability, and lower wear risk, rendering it more suitable for high-speed continuous industrial production. The sparse distribution, by contrast, is not conducive to high-efficiency continuous production.

3) When the spacing between paddy grain clusters is 0 mm, ultra-local high-stiffness zones induce contact pressure concentration, with the maximum contact pressure reaching 10.06 MPa, and the maximum von Mises stress is also relatively high at 5.44 MPa. Although a peak time difference buffering effect is present, the rubber rollers still face risks of shear fatigue and accelerated surface crack initiation. At spacings of 2 mm and 8 mm, by contrast, the peaks of maximum contact pressure and von Mises stress coincide with no buffering effect, significantly elevating the wear risk of the rubber rollers. The maximum contact pressure peaks at 13.85 MPa at a 2 mm spacing. Optimal mechanical performance is achieved at a 6 mm spacing, with the minimum maximum von Mises stress and the lowest risks of plastic yielding and uneven wear. Overall, the contact mechanical performance of the stacked paddy grain flow is inferior to that of the sparsely and

densely distributed paddy grain flows, and paddy grain stacking inevitably induces uneven wear of the rubber rollers.

4) The numerical simulation model established in this study is based on several necessary simplified mechanical assumptions. While these simplifications facilitate focusing on the core mechanism of "wear induced by uneven paddy grain flow" and ensure high computational efficiency, they inevitably introduce inherent limitations. Specifically, the model cannot accurately predict local extreme contact pressure values, the effects of paddy grain randomness, rubber material viscoelastic energy dissipation, and the long-term wear evolution processes of the rubber rollers. Additionally, the influences of dynamic environmental factors in actual industrial production are not considered.

To further improve the prediction accuracy and engineering applicability of the model, future research will focus on three key research directions: first, measuring the actual contact stress of the rubber rollers using a dedicated experimental platform to calibrate the key model parameters; second, introducing multi-scale coupling simulation methods, a nonlinear constitutive model for rubber materials, and realistic paddy grain morphologies to optimize the model and improve the authenticity of simulation results; third, establishing a comprehensive condition evaluation system for rubber rollers that integrates numerical simulation results and experimental verification data. Ultimately, this research will provide more reliable theoretical support and a scientific decision-making basis for the prevention and control of uneven wear of rubber rollers and the optimization of paddy grain hulling processing technologies in actual industrial production.

Acknowledgements

[References]

[1]   Shitanda D, Nishiyama Y, Koide S. Husking characteristics of short and long grain rice by rubber roll husker (part 1): Dynamic analysis of a single grain motion. Journal of the Japanese Society of Agricultural Machinery, 2001; 63(1): 55–63.

[2]   Yehia M E, Katab A R. Effect of hulling machines on hulling characteristics and quality of rice grains. Misr Journal of Agricultural Engineering, 2018; 35(1): 259–274.

[3]   Adetola O A, Akindahunsi D L. A review on performance of rice de-stoning machines. Journal of Engineering Research and Reports, 2020; 13(1): 1–11.

[4]   Yisa M G, Fadeyibi A, Katibi K K, Ucheoma O C. Performance evaluation and modification of an existing rice destoner. International Journal of Engineering Technologies, 2017; 3(3): 169–175.

[5]   Danjuma S B, Oke P K. Development of a domestic water medium rice de-stoning machine. Journal of Food and Nutrition, 2023; 2(1): 2836–2276.

[6]   Jia L L, Ruan J L. Discrete element simulation and experiment research of material flow in. Food & Machinery, 2016; 32(5): 91–93. (in Chinese).

[7]   Chen P Y, Jia F G, Liu H R, Han H L, Zeng Y, Meng X Y, et al. Effects of feeding direction on the hulling of paddy grain in a rubber roll huller. Biosystems Engineering, 2019; 183: 196–208.

[8]   Firouzi S, Alizadeh M, Minaei S. Effect of rollers differential speed and paddy moisture content on performance of rubber roll husker. International Journal of Natural & Engineering Sciences, 2010; 4(3): 37–42.

[9]   Chen P Y, Han Y L, Jia F G, Meng X Y, Xiao Y W, Bai S G. DEM simulations and experiments investigating the influence of feeding plate angle in a rubber-roll paddy grain huller. Biosystems Engineering, 2021; 201: 23–41.

[10] Fei J M, Feng W Y, Shen S H, Han Y L, Li A Q, Hao X Z, et al. Non-uniform milling caused by preferential orientation of rice grains in friction rice mills. Biosystems Engineering, 2023; 235(9): 15–30.

[11] Prabhakaran P, Ranganathan R, Muthu Kumar V, Rajasekar R, Devakumar L, Pal S K, et al. Review on parameters influencing the rice breakage and rubber roll wear in sheller. Archives of Metallurgy and Materials, 2017; 62: 1875–1880.

[12] Wang Z X, Wang W P, Song S Y. Simulation analysis of the influencing parameters on the shelling efficiency of rubber roller husker based on ADAMS. Food and Machinery, 2024; 39(12): 83–87. (in Chinese).

[13] Wu Z Y, Jin T, Liu X X, Zhang Z W, Zhao B B, Zhang Y H, et al. Research on the wear state detection and identification method of huller rollers based on point cloud data. Coatings, 2024; 14(9): 1209.

[14] Adisa A F, Mamah K C, Aderinlewo A A, Ismaila S O. Effectiveness of industrial rubber as roller material for rice processing machine. Agriculture and Natural Resources, 2020; 54(1): 98–104.

[15] Adisa A F, Eberendu O N, Aderinlewo A O, Kuye I S. Effectiveness of Teflon as roller material for a prototype rice processing machine. Agricultural Engineering International: CIGR Journal, 2016; 18(4): 107–118.

[16] Baker A, Dwyer-Joyce R S, Briggs C, Brockfeld M. Effect of different rubber materials on husking dynamics of paddy rice. Proceedings of the Institution of Mechanical Engineers, Part J: Journal of Engineering Tribology, 2012; 226(6): 516–528.

[17] Paramasivam P, Ranganathan R, Rathanasamy R, Kaliyannan G V, Palaniappan S K, Pal S K, et al. Experimental analysis on the technical behavior of carbon black filled rubber blends' rollers for rice husk removal application. Polimery, 2019; 64(1): 50–55.

[18] Alwan Alsharifi S K, Alaamer S A, Ajmi N, Kheiralipou K. Effect of husking machines and clearances on two rice cultivars. Agricultural Engineering International: CIGR Journal, 2024; 26(1): 222–240.

[19] Alsharifi Alwan S K, Arabhosseini A, Kianmeher M H, Kermani A M. Effect of moisture content, clearance and machine type on some qualitative characteristics of rice (Tarm Hashemi) cultivar. Bulgarian Journal of Agricultural Science, 2017; 23(2): 348–355.

[20] Alsharifi S K A. Effect of grain moisture content and machine clearance on mechanical damage of husked paddy. Agricultural Engineering International: CIGR Journal, 2022; 24(2): 137–142.

[21] Valentin L P. Exact solution method for contact problems: Hertzian contact. In: Li Q. Contact mechanics and friction: physical principles and applications. Beijing: Tsinghua University Press, 2019; pp.49–65.

[22] Zheng Z M, Zang M Y, Chen S H, Zhao C H. An improved 3D DEM-FEM contact detection algorithm for the interaction simulations between particles and structures. Powder Technology, 2017; 305: 308–322.

[23] Cheng M, Chen R B, Cao X Z. An equivalent design method for mechanical structure of rotor system of rubber roller huller. Journal of Henan University of Technology (Natural Science Edition), 2023; 44(3): 113–119. (in Chinese)

[24] Chen P Y. Study on the hulling mechanism of paddy grain in an rubber roll huller. Master dissertation, Harbin: Northeast Agricultural University. 2020; 58p. (in Chinese). doi: 10.27010/d.cnki.gdbnu.2020.000890

[25] Liu Y P, Zhang T, Liu Y. Calibration and experiment of contact parameters of rice grain based on discrete element method. Journal of Agricultural Science and Technology, 2019; 21(11): 70–76. (in Chinese)

[26] Genç O K, Kong Z, Keshtegar B, Thai D K. Blast-resistant design of reinforced concrete slabs with auxetic-shaped reinforcement layout. Buildings, 2024; 14(11): 3392.

[27] Prabowo A R, Ridwan R, Braun M, Song S, Ehlers S, Firdaus N, et al. Comparative study of shell element formulations as NLFE parameters to forecast structural crashworthiness. Curved and Layered Structures, 2023; 10(1): 20220217.

[28] Liu W. Testing of wheel-rail contact patch and contact pressure analysis. Master dissertation, Beijing: Beijing Jiaotong University. 2014; 98p. (in Chinese)

[29] Huang F Z. Concept of thermal contact resistance and influences of hysteresis and tangential stress. Journal of Northwest University (Natural Science Edition), 1993; 23(2): 119–125. (in Chinese)